N08600014

UNIVERSITY OF OSLO

INSTITUTE OF PHYSICS

REPORT SERIES

ISSN 0332-5571

STATISTICAL γ-DECAY IN s-d SHELL NUCLEI

M. Guttormsen, A. Ataç, F. Ingebretsen,
S. Messelt, J. Olsen, T. Ramsøy, J. Rekstad
and L.A. Rönning
Institute of Physics, University of Oslo, Oslo
Norway

G. Løvhøiden, T. Rødland and T.F. Thorsteinsen
Institute of Physics, University of Bergen, Bergen,
Norway

OUP--
Report 85-27 Received 4/12-85

Statistical γ-Decay in s-d Shell Nuclei

M. Guttormsen, A. Ataç, F. Ingebretsen, S. Messelt,
J. Olsen, T. Ramsøy, J. Rekstad and L.A. Rønning

Institute of Physics, University of Oslo, Oslo, Norway

G. Løvhøiden, T. Rødland and T.F. Thorsteinsen

Institute of Physics, University of Bergen, Bergen, Norway

Abstract

The γ-decay following the $^{27}Al(\tau,\alpha)$, $^{27}Al(\tau,\tau)$ and $^{27}Al(\tau,t)$ reactions has been studied using E_τ = 45 MeV. For all three reactions a maximum mean γ-ray multiplicity of $\langle M_\gamma \rangle = 1.8 \pm 0.2$ is observed, in good agreement with the Fermi gas model. The variation of $\langle M_\gamma \rangle$ with excitation energy for the $^{27}Al(\tau,\tau)^{27}Al$ reaction, however, shows considerable deviations from the decay pattern expected for a statistical system. From a comparison with other reaction channels, we suggest that the selectivity in the excitation of states in the inelastic process is responsible for this non-statistical pattern.

NUCLEAR REACTIONS $^{27}Al(\tau,\alpha)$, $^{27}Al(\tau,\tau)$ and $^{27}Al(\tau,t)$, E = 45 MeV; measured $\sigma(E)$, E_γ, I_γ; $\tau\gamma,\alpha\gamma,t\gamma$-coin. Deduced γ-ray multiplicity. Ge(Li), NaI(Tl), Si detectors. Fermi gas model analysis.

1. Introduction

Recently, the statistical and thermodynamical aspects of nuclear matter have received new interest (1-4). At low excitation energies the nuclear level scheme is determined by the specific structure of single particle orbitals. However, already a few MeV above the yrast line the nuclear level density is so high that statistical concepts like temperature and entropy can be used in the description.

Previously (4,5), it has been demonstrated that the number of γ-rays participating in the decay of heated nuclei is overall well described by the Fermi gas model for mass numbers $A \sim 60$, $A \sim 120$ and $A \sim 160$. The model reproduces both the magnitude and the variations in the γ-ray multiplicity as a function of excitation energy. In the present work these investigations have been extended to nuclei in the s-d shell, which may be considered as a limiting case for a statistical description of the decay process.

In sect. 2 we describe the experimental set-up and the particle-gamma coincidence method used. The nuclear reaction mechanisms and cross-sections are discussed in sect. 3. In sect. 4 the experimental results are compared with Fermi gas model calculations. Finally, concluding remarks are given in sect. 5.

2. Experimental method

The experiment was performed using 45 MeV ^{7}Li-ions from the MC-35 cyclotron at the University of Oslo. A self supporting ^{27}Al foil with a thickness of 2mg/cm^2 was used as target.

The set-up was designed to measure γ-rays in coincidence with outgoing charged particles from the reaction. The particles were detected with four silicon ΔE-E telescopes at $\theta=50^{\circ}$ with respect to the incident beam direction. The counters had thicknesses of 150 μm and 3000 μm, respectively giving a good separation of α, τ and t particles. In order to obtain sufficient count rates the telescopes were placed as close as 4 cm from the target. The large solid angle in this geometry resulted in a particle resolution of 0.7 MeV.

The γ-rays were detected with five 5"x5" NaI counters and one Ge(Li) counter. Lead collimators in front of the NaI counters prevented γ-rays from entering the peripheral parts of the crystals. The probability of cross-talk between two adjacent counters were measured to be 0.05% for 1.3 MeV γ-rays.

In the coincidence mode it was required that one and only one telescope fired in coincidence with one or more γ-ray counters. The particle and γ-ray energies were recorded event by event on magnetic tapes together with coincidence time information. In addition, every tenth singles particle detected was recorded on the tape for the production of normalized singles particle spectra.

3. Experimental results

In the present work we focus on the gross structure of the nuclei ^{24,25}Mg, ^{26,27}Al and ^{27}Si produced in the reactions. Information on the detailed level structure and decay properties can be found elsewhere (6).

Particle spectra from the (τ,α), (τ,τ) and (τ,t) reactions on ^{27}Al are displayed in figs. 1-3. The upper part shows the

singles spectrum of the outgoing particles. The middle part shows the same spectrum measured in coincidence with at least one γ-ray ($E_\gamma > 0.45$ MeV) detected by the NaI counters. The lower spectrum, named multiplicity, is constructed by dividing the coincidence spectrum (N_c) with the singles spectrum (N_s) channel by channel:

$$\langle M_\gamma(E) \rangle = \frac{N_c(E)}{\Omega(1.0 \cdot N_s(E))} \qquad (1)$$

where E is the particle energy and $\Omega = 2.68\%$ is the total efficiency of the NaI counters. An energy threshold of 0.45 MeV for the NaI counters was chosen in order to obtain an almost constant total detection probability as a function of E_γ.

The $^{27}Al(\tau,\alpha)^{24}Al$ and the $^{27}Al(\tau,t)$ ^{27}Si reactions have increasing cross-sections with increasing excitation energies. The $^{27}Al(\tau,\tau)^{27}Al$ spectrum is dominated by the elastic scattering and has a close to constant cross-section at higher excitation energies. The spectrum of inelastically scattered particles observed in coincidence with γ-rays shows large variations in the cross-section. This is a measure of variations in the γ-ray multiplicity and is connected to the onset of proton emission above the proton binding energy.

The particle spectra can be studied by gating on specific γ-rays in residual nuclei after subsequent particle emission. Figures 4 and 5 show such spectra. Due to the large positive Q-value of 7.52 MeV for the (τ,α) reaction both the proton and the proton-neutron evaporations are observed in this case. The α-particles giving rise to states in ^{24}Al are identified with energies between 42 and 47 MeV. Since the total multiplicity is found to be $\langle M_\gamma \rangle < 2$ (see fig. 1) and we already have utilized one transition (the 829 keV transition) in the gating procedure, the 1^+ state in ^{24}Al is essentially populated by direct γ-ray

feeding. This γ-ray transition is expected to be of statistical dipole type (7,8), which gives a narrow spin window of $|\Delta I| < 1$. Thus, the α-particle distribution represents states with an average spin $\langle I \rangle$ close to unity. Above the proton binding energy of the ^{26}Al nucleus, the neighbouring ^{25}Mg nucleus is populated, as seen in fig. 4. The α-particle distribution related to the population of the $1/2^+$(585 keV) level in ^{25}Mg has more than a 5 MeV overlap with the α-particles leading to ^{24}Mg. This extended range of α-particle energies in ^{25}Mg is caused by fast protons leaving ^{26}Al.

With our beam energy only one proton is emitted in the (τ,τ) and (τ,t) reactions. Figure 5 shows an interesting situation where the τ-particles from ^{27}Al and ^{24}Mg overlap in energy. Here, even 5 MeV above the proton binding energy (B_p = 8.27 MeV) the $7/2^+$ (2163 keV) level in ^{27}Al is populated. This means that the γ-decay following inelastic scattering competes favourably with proton emission.

The favoured γ-decay is also apparent for states with other spin assignments. Figure 6 shows τ-particle spectra obtained with gates on prominent γ-ray transitions in ^{27}Al. All spectra reveal a significant particle yield above the proton binding energy.

From the discussion of the particle spectra we conclude that the ^{27}Al nucleus produced in the (τ,τ) reaction exhibits the most prominent peak structure in the spectra. An inspection of fig. 6 also shows that states with the lowest spins, in particular the $3/2^+ \rightarrow 5/2^+$ gate, have outstanding particle groups in the spectra. The ^{27}Si mirror nucleus produced in the charge-exchange (τ,t) reaction seems to yield a spectrum that is much closer to a continuum spectrum, as shown in fig. 3. Unfortunately, an

analysis of the data pertinent to this nucleus is difficult due to insufficient statistics. The odd-odd ^{28}Al nucleus from the (τ,α) reaction as well as the residual nuclei following particle emissions (see fig. 1) also yield more continuous particle spectra.

4. The γ-decay and comparison with the Fermi gas model

In the following the question to what extent the γ-decay follows statistical laws is discussed, by comparing with Fermi gas model predictions.

The probability for emission of a γ-ray with energy E_γ from an excitation energy E_x is given by

$$P(E_x,E_\gamma) \propto E_\gamma^n \cdot \rho(E_x - E_\gamma) \ , \qquad (2)$$

where the level density ρ is computed for the excitation region after the γ-emission. Values of the parameter n ranging from n = 3-6 have been suggested (9-11), where the lower limit of n ($2\lambda + 1 = 3$) is based on general radiation theory for dipole transitions. However, one expects larger effective values due to structural overlap factors originating from the tail of the giant dipole resonance. In this work we have chosen n = 5.

To evaluate the level density the independent-particle Fermi gas model with pairing is used, as described by Richter (12). The density at an excitation energy E_x for spin I of both parities reads

$$\rho(E_x,I) = \frac{\hbar^3(2I+1)}{24\cdot 2^{1/2}(a\theta)^{3/2}t^4} \times \exp\{[a(E_x - E_\Delta)]^{1/2} - [\frac{I(I+1)}{2\sigma^2}]\} \ , \qquad (3)$$

where the level density parameter a is estimated to be $A/8$ MeV^{-1} and the moment of inertia Θ to be $0.0137\ A^{5/3}\ \hbar^2$ MeV^{-1}. E_x is the excitation energy and E_Δ measures the energy difference between the effective and true ground band state. This parameter is taken to be 0 for odd-odd nuclei and $\Delta = 12\ A^{-1/2}$ MeV for odd-even nuclei. The spin cut-off parameter σ^2 is $\Theta t/\hbar^2$, where the thermodynamical temperature t fulfills the equation

$$E_x - E_\Delta = at^2 - t \ . \qquad (4)$$

For the lowest excitation region ($E_x < 1$ MeV) we have used a constant level density corresponding to experimentally known number of levels.

The computational technique is based on Monte Carlo simulation where we evaluate at each step in the decay the expression

$$F(E_x^i, E_\gamma^i) = \int_0^{E_\gamma^i} P(E_x^i, E_\gamma)\,dE_\gamma \Big/ \int_0^{E_x^i} P(E_x^i, E_\gamma)\,dE_\gamma \ . \qquad (5)$$

From a random number f between 0 and 1 the γ-ray energy E_γ corresponding to $F = f$ is chosen. The excitation energy in eq. (5) is replaced by $E_x^{i+1} = E_x^i - E_\gamma^i$ and the procedure is repeated until the ground state is reached. The γ-decay is then simulated by a series of such calculations and the γ-ray energies are accumulated in various spectra.

The experimental γ-ray multiplicities as a function of excitation energy is shown in fig. 7. The solid curves represent the results of the Monte Carlo simulation. In the ^{26}Al and ^{27}Si cases the Fermi gas model describes the observed multiplicities

for excitation energies down to 2 MeV. At the proton binding energy B_p both experimental curves show the same abrupt decrease. This deviation from the Fermi gas model is due to the emission of a proton. The residual nucleus is populated at low excitation energies and is responsible for the observed low γ-ray multiplicity.

The multiplicity curve for the (τ,τ) reaction shows a step-like behaviour quite at variance with the predictions of the Fermi gas model. Only in the energy region 5 to 8 MeV is the value of the multiplicity in accordance with the model. The slow fall in multiplicity above $E_x = B_p$ verifies that a substantial part of the decay proceeds through γ-ray emission instead of proton emission.

From the multiplicity measurements we learn that on the average only one or two γ-transitions participate in the decay. In the case of two coincident γ-rays, the first one will have a much higher energy than the second one. This is a consequence of the low densities of levels in these nuclei. An estimate can be derived by assuming a constant level density giving a decay probability proportional to E_γ^n (see eq. 2). For $M_\gamma = 2$ events we calculate $(n + 1)/(n + 2) \cdot E_x$ and $1/(n+2) \cdot E_x$ as the γ-ray energies of the first and second emitted γ-ray, respectively.

The lower part of fig. 8 shows γ-ray spectra from simulations of cascades starting from the region of $E_x = 4.5 - 5.5$ MeV. A striking feature of the calculated spectra is the low number of γ-rays with energy around $E_x/2$. The calculations predict an intensity reduction of a factor of ten compared to the maximum which is found around $E_\gamma \approx 6/7\ E_x = 4.3$ MeV. In the spectra folded by the NaI response function this intensity

reduction remains as a fingerprint of statistical γ-decays in these low level density systems. The experimental γ-ray spectra are shown in the upper part of fig. 8. While for ^{27}Al there is no sign of intensity loss in the 2-3 MeV region, the ^{26}Al nucleus indeed reveal some drop in intensity.

The low multiplicity in our reactions can be utilized in a new method for producing γ-ray spectra almost free from compton scattering. Table 1 shows from a simulation at E_x = 5 MeV that M_γ = 3 events in the decay are improbable. The multiplicity distribution is very narrow and centered around 1.5. Thus, if we require that two γ-rays have been detected, it is highly probable that they constitute the total decay. Therefore, full-energy detected events can be sorted out by requiring $E_{\gamma 1} + E_{\gamma 2} \sim E_x$.

In fig.9 γ-ray spectra from various excitation regions in ^{26}Al and ^{27}Al are shown together with the Fermi gas predictions. A broad gate of 1.5 MeV was used in the sorting procedure. To increase the statistics the γ-ray energies E_γ from both detectors are incremented in the same spectrum and the spectrum is symmetrized around $E_x/2$ by also incrementing $E_x - E_\gamma$ for each E_γ.

The shapes of the ^{26}Al spectra are generally in good agreement with the predictions, whereas in the ^{27}Al case a statistical behaviour is first apparent at the highest excitation energies.

5. Summary and conclusions

The γ-decay from the ^{27}Al$(\tau,\alpha)^{26}$Al, ^{27}Al$(\tau,\tau)^{27}$Al and ^{27}Al$(\tau,t)^{27}$Si reactions has been studied and compared with the Fermi gas model. The observed γ-ray multiplicities for

^{26}Al and ^{27}Si are found to be well described within the model. However, in the inelastic ^{27}Al case the multiplicity curve has a step-like behaviour as function of excitation energy. This indicates that certain groups of states are favoured in the γ-decay. In regions above the proton binding these favoured γ-transitions even compete significantly with the proton emission.

The γ-ray NaI spectra have been examined for particle-γ and particle-γ-γ events. The Fermi gas model predicts a loss in γ-ray intensities around $E_\gamma = E_x/2$. Indeed, this feature is seen in the spectra for ^{26}Al, but not for ^{27}Al.

The deviation from a statistical decay pattern for ^{27}Al is due to the reaction used. The inelastic scattering is likely to populate vibrational states. The following γ-decay is fast and competes strongly with proton emission. Thus, provided that the γ-decay occurs within the relaxation time of the system, states of vibrational character will be populated in the proceeding γ-cascade. Such a selectivity of states both in the reaction channel and in the γ-decay could explain the non-statistical behaviour found in the ^{27}Al$(\tau,\tau)^{27}$Al reaction.

Table 1.

Theoretical γ-ray multiplicity distribution at E_x = 5 MeV

Nucleus	Probability (%)			$\langle M_\gamma \rangle$
	M_γ=1	2	3	
^{26}Al	46	50	4	1.6
^{27}Al	50	48	2	1.5

References

1. T. Ramsøy, J. Rekstad, M. Guttormsen, A. Henriquez, F. Ingebretsen, T. Rødland, T.F. Thorsteinsen and G. Løvhøiden, Nucl. Phys. A438, 301 (1985)

2. T. Ramsøy, J. Rekstad, A. Henriquez, F. Ingebretsen, M. Guttormsen, E. Hammarén and T.F. Thorsteinsen, Nucl. Phys. A414, 269 (1984)

3. O. Civitarese and A.L. De Paoli, Z. Phys. A321, 473 (1985)

4. J. Rekstad, A. Henriquez, F. Ingebretsen, E. Midttun, B. Skaali, R. Øyan, J. Wikne, T. Engeland, T.F. Thorsteinsen, E. Hammaren and E. Liukkonen, Phys. Scripta T5, 45 (1983)

5. J.H. Degnan, B.L. Cohen, G.R. Rao, K.C. Chan and L.Shabason, Phys. Rev. 18, 2255 (1973)

6. C.M. Lederer and V.S. Shirley, ed. Table of isotopes, 7th ed. (Wiley, New York, 1978)

7. S.J. Feenstra, J. Van Klinken, P.J. Pijn, R. Janssens, C. Michel, J. Steyaert, J. Vervier, K. Cornelis, H. Huyse and G. Lhersonneau, Phys. Lett. B0B, 183 (1979)

8. A. Henriquez, J. Rekstad, F. Ingebretsen, M. Guttormsen, K. Eldhuset, B. Normoen, T. Ramsøy, R. Renstrøm-Pedersen, R.M. Aasen, T.F. Thorsteinsen and E. Hammarén, Phys. Lett. 130B, 171 (1983)

9. S.M. Sie, J.O. Newton and R.M. Diamond, Nucl. Phys. A367, 176 (1981)

10. J.M. Blatt and V.F. Weisskopf, Theoretical Nuclear Physics (Wiley, New York, 1967), p. 583

11. R.J. Liotta and R.A. Sørensen, Nucl. Phys. A297, 136 (1978)

12. A. Richter, Nuclear Spectroscopy and Reactions, B, ed. J. Cerny (Academic Press, New York, 1974), p. 343

Figure captions

Fig. 1. Singles α-spectrum, α-particles in coincidence with γ-rays (E_γ > 0.45 MeV in the NaI counters) and γ-ray multiplicity spectrum.

Fig. 2. Singles τ-spectrum, τ-particles in coincidence with γ-rays (E_γ > 0.45 MeV in the NaI counters) and γ-ray multiplicity spectrum.

Fig. 3. Singles t-spectrum, t-particles in coincidence with γ-rays (E_γ > 0.45 MeV in the NaI counters) and γ-ray multiplicity spectrum.

Fig. 4. Alpha-spectra obtained by gating on various γ-ray transitions in the residual nuclei (transitions indicated in level schemes).

Fig. 5. Tau-spectra obtained by gating on various γ-ray transitions in the residual nuclei (transitions indicated in level schemes).

Fig. 6. Tau-spectra obtained by gating on various transitions in ^{27}Al (see level scheme). The lower spectrum represents the projection of τ-particles in coincidence with all γ-rays.

Fig. 7. Gamma-ray multiplicity spectra from the ^{27}Al(τ,αγ), ^{27}Al(τ,τγ) and ^{27}Al(τ,tγ) reactions. The proton binding energies are indicated by arrows.

Fig. 8. Gamma-ray spectra from 4.5-5.5 MeV excitation energy. The theoretical unfolded spectra have been calculated assuming Fermi gas conditions. The spectra in the middle part have been folded using the NaI response function. The upper spectra are the experimental raw spectra measured with the NaI counters.

Fig. 9. Gamma-ray spectra as function of excitation energies in

^{24}Al and ^{27}Al. The solid curves represent the Fermi gas predictions.

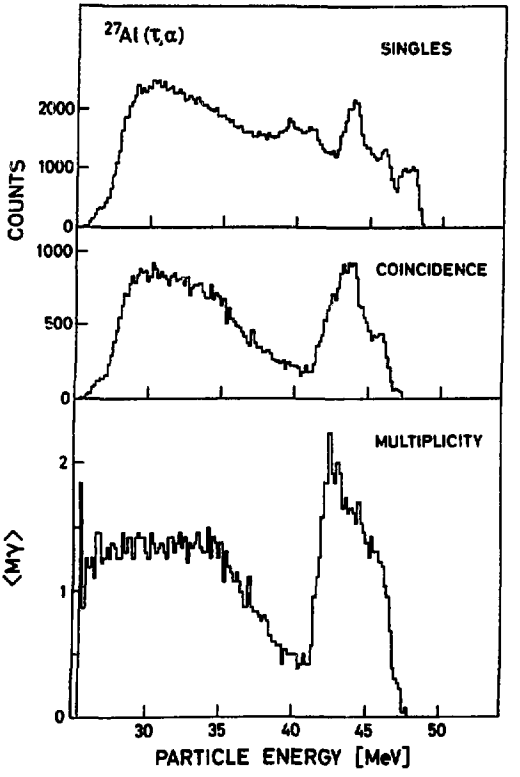
^{27}Al (τ,α)
SINGLES
COUNTS
2000
1000
0
COINCIDENCE
1000
500
0
MULTIPLICITY
<MY>
2
1
0
30
35
40
45
50
PARTICLE ENERGY [MeV]

Fig. 1

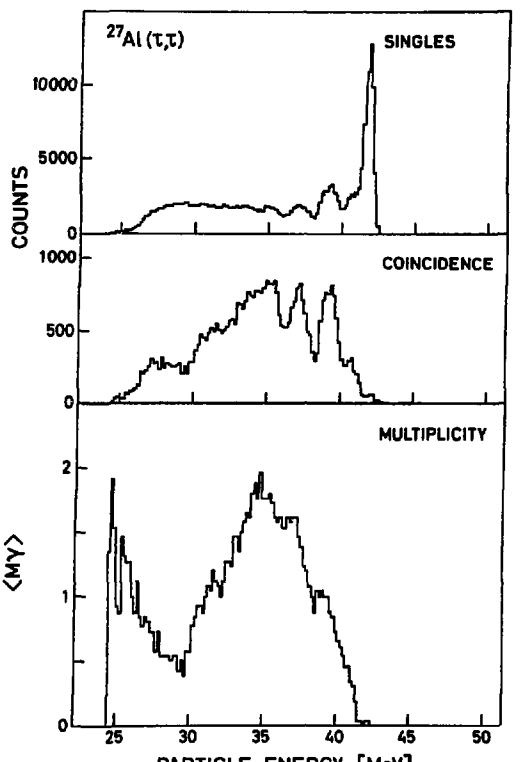
^{27}Al (τ,τ)
SINGLES
COINCIDENCE
MULTIPLICITY
COUNTS
10000
5000
0
1000
500
0
2
1
0
<MY>
25
30
35
40
45
50
PARTICLE ENERGY [MeV]

Fig. 2

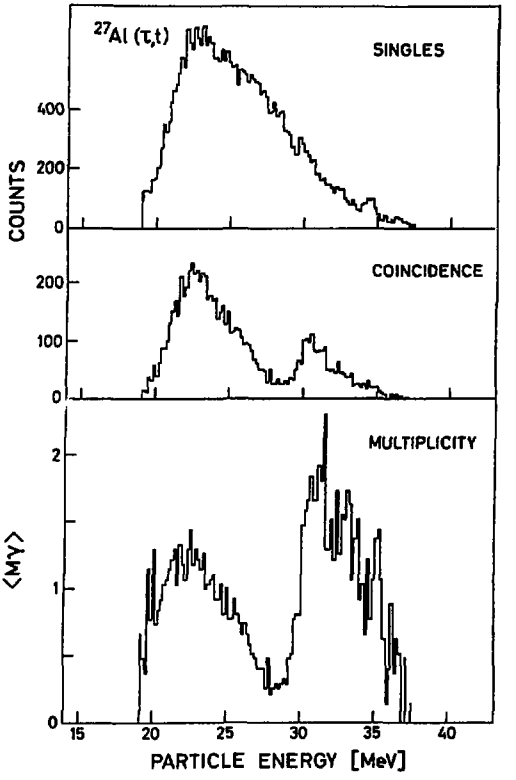
^{27}Al (τ,t)
SINGLES
COINCIDENCE
MULTIPLICITY
COUNTS
<Mγ>
400
200
0
200
100
0
2
1
0
15
20
25
30
35
40
PARTICLE ENERGY [MeV]

Fig. 3

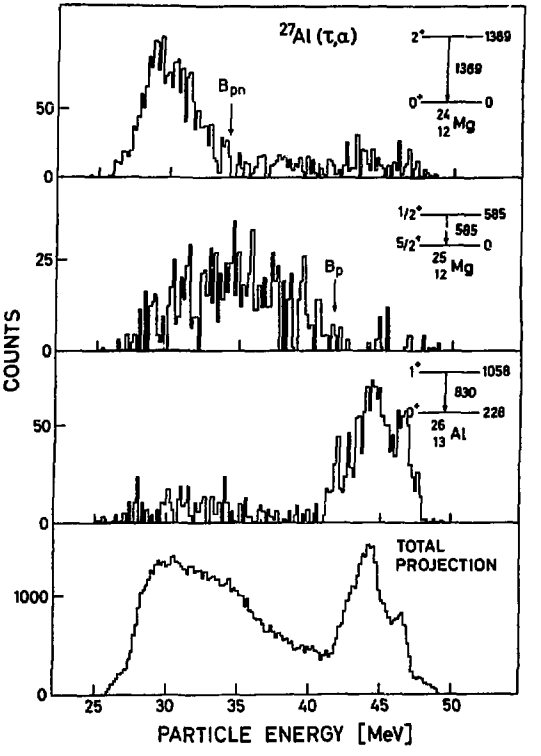
^{27}Al (τ,α)
B_{pn}
B_p
2⁺ 1369
1369
0⁺ 0
$^{24}_{12}$Mg
1/2⁺ 585
585
5/2⁺ 0
$^{25}_{12}$Mg
1⁺ 1058
830
0⁺ 228
$^{26}_{13}$Al
TOTAL PROJECTION
COUNTS
PARTICLE ENERGY [MeV]

Fig.4

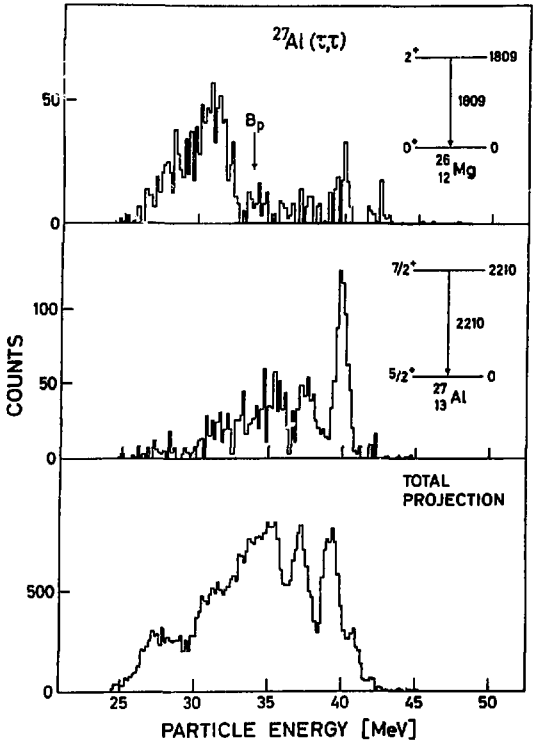
^{27}Al (τ,τ)
2⁺ 1809
1809
0⁺ 0
$^{26}_{12}$Mg
B_p
7/2⁺ 2210
2210
5/2⁺ 0
$^{27}_{13}$Al
TOTAL PROJECTION
COUNTS
50
0
100
50
0
500
0
25
30
35
40
45
50
PARTICLE ENERGY [MeV]

Fig. 5

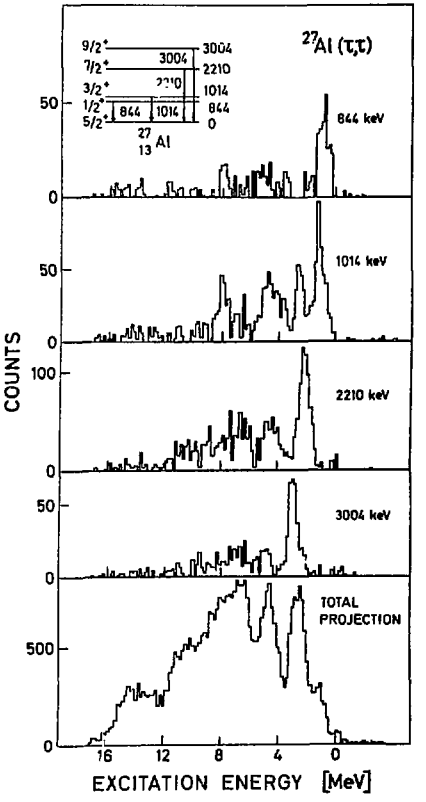
^{27}Al (τ,τ)
9/2+
7/2+
3/2+
1/2+
5/2+
3004
2210
1014
844
0
844
1014
$^{27}_{13}$Al
844 keV
1014 keV
2210 keV
3004 keV
TOTAL PROJECTION
COUNTS
EXCITATION ENERGY [MeV]
16
12
8
4
0

Fig. 6

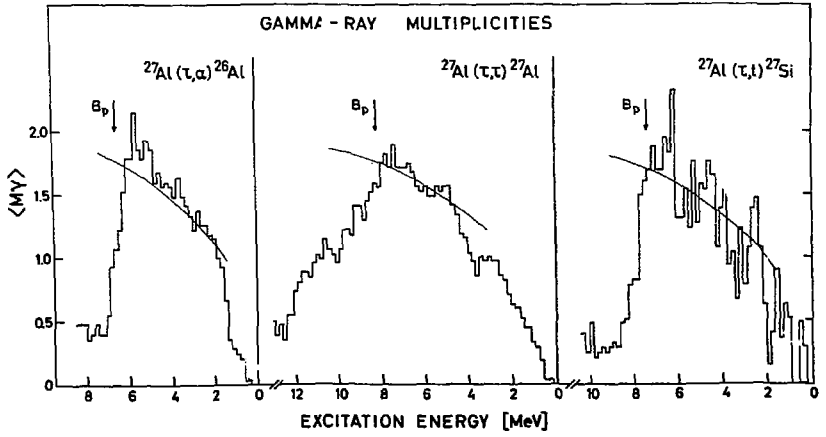
GAMMA - RAY MULTIPLICITIES
^{27}Al (τ,α) ^{26}Al
^{27}Al (τ,τ) ^{27}Al
^{27}Al (τ,t) ^{27}Si
B_p
B_p
B_p
⟨Mγ⟩
2.0
1.5
1.0
0.5
0
8 6 4 2 0
12 10 8 6 4 2 0
10 8 6 4 2 0
EXCITATION ENERGY [MeV]

Fig. 7

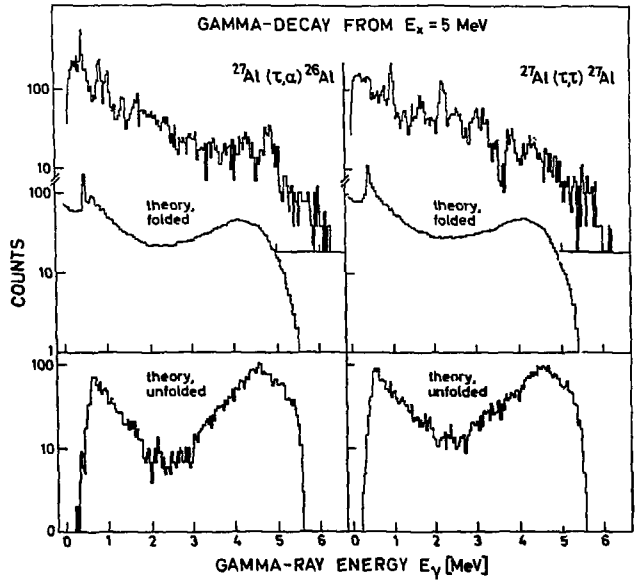
GAMMA-DECAY FROM E_x = 5 MeV
^{27}Al (τ,α) ^{26}Al
^{27}Al (τ,τ) ^{27}Al
theory, folded
theory, unfolded
COUNTS
GAMMA-RAY ENERGY E_γ [MeV]

Fig. 8

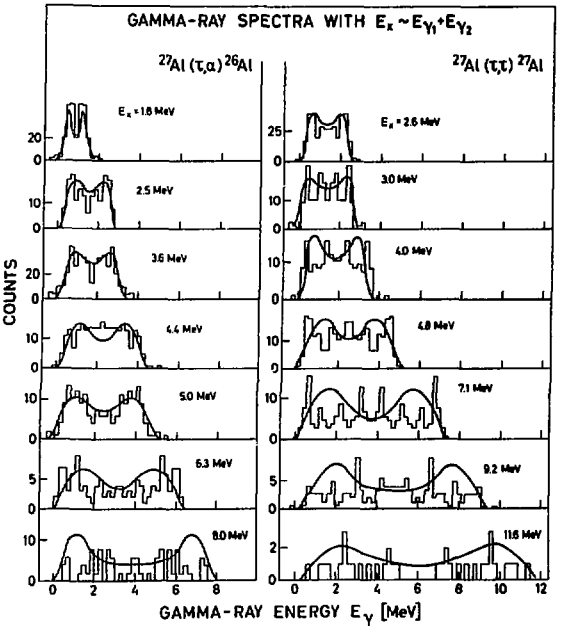
GAMMA-RAY SPECTRA WITH $E_x \sim E_{\gamma_1}+E_{\gamma_2}$
$^{27}Al\,(\tau,\alpha)\,^{26}Al$
$^{27}Al\,(\tau,\tau)\,^{27}Al$
E_x = 1.8 MeV
2.5 MeV
3.6 MeV
4.4 MeV
5.0 MeV
6.3 MeV
8.0 MeV
E_x = 2.6 MeV
3.0 MeV
4.0 MeV
4.8 MeV
7.1 MeV
9.2 MeV
11.6 MeV
COUNTS
GAMMA-RAY ENERGY E_γ [MeV]

Fig. 9